Original Article

MOLECULAR METABOLISM

Characterization of LY3324954 a long-acting glucagon-receptor agonist

William Roell[1], Tamer Coskun[1], Teayoun Kim[2], Libbey O'Farrell[1], Jennifer A. Martin[1], Shelly Nason[2], Jasmin Hernandez-Alamillo[2], Saidharshana Dhantu[2], Daniel J. Drucker[3], Kyle W. Sloop[1], James P. Steele[1], Jorge Alsina-Fernandez[1,**], Kirk M. Habegger[2,*]

ABSTRACT

Glucagon is a crucial regulator of glucose and lipid metabolism as well as whole-body energy balance. Thus, modulation of glucagon receptor (GCGR) activity in the context of single-molecule multi-receptor co-agonists has become an emerging therapeutic target against obesity and obesity-associated metabolic dysfunction. To better elucidate the role of GCGR-signaling when paired with incretin receptor signaling or on its own, we developed, LY3324954, a GCGR agonist with improved potency and selectivity as compared to the native glucagon peptide. LY3324954 also exhibited extended pharmacokinetic (PK) profile in DIO mice, rats, dogs, and monkeys. When administered every 72 h, LY3324954 treatment stimulated transient glucose and insulin excursions in lean mice. In diet-induced obese mice, LY3324954 treatment stimulates energy expenditure, weight loss, and a reduction of adiposity in a dose-dependent manner. Benefit to whole-body lipid homeostasis was likewise observed in these mice. Taken together, these studies characterize a long-acting and potent GCGR-agonist and its regulation of glucose and lipid metabolism as well as whole-body energy balance following both acute and chronic treatment in mice.

Keywords Glucagon; Insulin secretion; Glucose homeostasis; Diabetes; Obesity

1. INTRODUCTION

Glucagon (GCG) is a 29-amino acid peptide released from α-cells of the pancreatic islet [1,2]. Its stimulation of hepatic glycogenolysis and gluconeogenesis has characterized glucagon as a counterregulatory hormone [1,2]. Accordingly, acute, high-dose glucagon injections are life-saving therapy against insulin-induced hypoglycemia. However, glucagon also regulates metabolic actions (as reviewed in [1]) including, amino acid catabolism, lipolysis [3–8], ketogenesis [9], fatty acid oxidation [10,11], satiety [12–16], thermogenesis [17,18], energy expenditure [19,20], and bile acid metabolism [21,22].

Glucagon-mediated improvements in lipid and energy metabolism would be of great value to patients with the metabolic syndrome. Consistent with these actions, the addition of glucagon receptor (GCGR) agonism to incretin hormones in long acting, single molecule, multi-receptor co-agonists show superior therapeutic efficacy in metabolically compromised rodent models as well as early phase clinical trials [23–27]. Importantly, these compounds which contain full GCGR-agonism, lack GCGR-associated hyperglycemic side-effects due to the engagement of GLP-1R and GIPR when studied in obese animals [23–27]. However, GCGR activity has long been associated with diabetes and obesity-associated glucose dysregulation [28]. Thus, it is important to optimize GCGR agonists to maximize metabolic and weight loss benefits while minimizing impairments to glucose homeostasis.

Emerging evidence supports that glucagon's metabolic actions may not exclusively counteract insulin action [29–31]. We and others have reported enhanced insulin sensitivity following glucagon or GCGR-agonism [29,30,32,33]. Glucagon also acts in an incretin manner, enhancing glucose-stimulated insulin secretion via direct effects on the pancreatic beta-cell [29,34,35]. Thus, while GCGR-signaling clearly augments the anti-obesity effects of incretin-based therapies, it may concurrently benefit insulin sensitivity and secretion. Moreover, a deeper understanding of the metabolic effects stimulated by long-acting agonists will be important to optimize these molecules for maximum energetic benefits while minimizing impairments to glucose homeostasis.

Data herein describes the preclinical validation of a novel GCGR-agonist, LY3324954, in lean and diet-induced obese mice. This peptide is a glucagon analog with modifications to enhance PK profile, stability in solution formulation, receptor specificity, and receptor engagement. Thus, this molecule represents a new tool to interrogate the physiology induced by protracted GCGR-agonism. Moreover, these studies may inform the biology shaped by therapies that engage GCGR-signaling.

[1]Lilly Research Laboratories, Indianapolis, IN, USA [2]Comprehensive Diabetes Center and Department of Medicine - Division of Endocrinology, Diabetes and Metabolism, University of Alabama at Birmingham, Birmingham, AL, USA [3]Department of Medicine, Lunenfeld-Tanenbaum Research Institute, Mt. Sinai Hospital, University of Toronto, USA

*Corresponding author. Department of Medicine - Endocrinology, Diabetes & Metabolism, University of Alabama at Birmingham Birmingham, AL, 35294, USA. E-mail: kirkhabegger@uabmc.edu (K.M. Habegger).

**Corresponding author. Eli Lilly and Company, Indianapolis, IN, 46285, USA. E-mail: alsina-fernandez_jorge@lilly.com (J. Alsina-Fernandez).

Received September 12, 2024 • Revision received November 8, 2024 • Accepted November 18, 2024 • Available online xxx

https://doi.org/10.1016/j.molmet.2024.102073

Original Article

2. MATERIALS & METHODS

2.1. Animal models

All studies were approved by and performed according to the guidelines of the Institutional Animal Care and Use Committee of the University of Alabama at Birmingham or of Eli Lilly and Company, and the Guide for the Use and Care of Laboratory Animals by the National Institutes of Health. Mice were single or group-housed on a 12:12-h light–dark cycle (light on from 0600 to 1800 h) at 22 °C in constant humidity with free access to food and water, except as noted. *Gcgr*-floxed mice were generated as previously described [29,36]. AAV8-TGB-iCre (2×10^{11} GC/mouse, no. VB1724; Vector BioLabs) was used to establish adult inducible, hepatic *Gcgr* knockout (i$Gcgr^{\Delta Liver}$ mice). $2*10^{11}$ genome copies (GC) per mouse of AAV-Cre or AAV-eGFP ($Cre^{Thryoxine\text{-}binding\ globulin}$;VB1743; Vector BioLabs) were induced via retro-orbital delivery and treatment was started 14d after induction. C57Bl/6 mice for studies detailed in Figures 1, 4–6, and Supplemental Fig. 2 were obtained from Taconic (Cambridge City, Indiana) and maintained in Eli Lilly and Co. facilities on high fat diet (HFD, Teklad D95217, 39.7 kcal% fat) with a 12:12-h light–dark cycle (light on from 2200 to 1000 h) at 24 °C in constant humidity with free access to food and water. C57Bl/6J mice for studies detailed in Figures 2 and 3, and Supplemental Fig. 3 were obtained from Jackson Labs and maintained in UAB facilities. Mice for Figures 2 and 3 were fed a standard chow (Teklad LM-485, 5.6% fat) while mice for Supplemental Fig. 3 were fed HFD with sucrose (D12331 Research Diets, 58.0 kcal% fat) for 12w to establish DIO.

2.2. Peptides

Insulin (Humulin® R) was obtained from Eli Lilly and Co. GCGR agonist, IUB288, was synthesized as previously described [37]. GCGR agonist, LY3324954, was synthesized at Eli Lilly and Company using Fmoc/tBu solid-phase peptide synthesis (SPPS) methods and solubilized in 20 mM Tris–HCl buffer at pH 8.0.

2.3. Pharmacokinetic analyses

The pharmacokinetics of LY3324954 were characterized in DIO mice, rats, dogs, and monkeys following a single subcutaneous administration. Plasma samples were analyzed for LY3324954 using a qualified liquid chromatography/mass spectroscopy method (LC/MS) at Q2 Solutions (Ithaca, NY, USA). LY3324954 and an analog internal standard were extracted from plasma by protein precipitation. A Thermo Q-Exactive, high resolution instrument, with a Supelco Discovery BioWide Pore C5-3 3 μm, 5 × 0.1 cm column were combined to allow for LC/MS detection. The range of quantification was from 10 nM to 1000 nM.

2.4. Cell based assays

Whole cell cAMP assays were performed in HEK293 cells expressing either the human or mouse GCGR as previously described [27]. The rat GCGR cAMP experiments were performed similar to assays previously reported for the mouse GCGR [27], albeit using HEK293 cells stably expressing the rat receptor (NP_742088). Briefly, cell lines were incubated for 30min with LY3324954 or controls in growth media supplemented with casein or HSA (1.0%) and intracellular cAMP was quantitatively determined. The amount of cAMP (nM) generated per well was converted to percent of the maximal response observed with either GCG, GLP-1(7–36)NH2, or GIP(1–42)NH2. Hepatocyte glucose output studies were performed using human induced pluripotent stem cell derived hepatocytes (Cellular Dynamics) as previously described [27].

2.5. Glucose tolerance tests

Glucose tolerance tests (GTT) were performed in 5 h fasted mice by i.p. injection of glucose (2 g/kg, 25% wt/vol D-glucose [Sigma] in 0.9% wt/vol saline). Blood glucose was determined by Contour glucometer (Ascensia Diabetes Care, 9545C).

2.6. Body composition and indirect calorimetry

Body weight and food intake measurements were collected twice a week. Body composition was measured using magnetic resonance spectroscopy (EchoMRI, Echo Medical Systems). Combined indirect calorimetry was conducted as previously described (TSE Systems, Chesterfield, MO) [27]. Briefly, animals were placed in TSE PhenoMaster/LabMaster calorimeter for 3 days of acclimation and all the experiments were performed at (27 °C). Daily water and food intake were measured via the PhenoMaster/LabMaster system. Heat and respiratory exchange ratio (RER) were measured by indirect calorimetry using an open-circuit calorimetry system. RER is the ratio of the volume of CO_2 produced (VCO_2) to the volume of O_2 consumed (VO_2). Heat was calculated with full body weight considered:

$$VO_2 = \text{FlowML} \times (V1+V2)/\text{N2Ref} \times \text{Animal weight} \times 100)$$

$$VCO_2 = \text{FlowML} \times dCO_2/\text{Animal weight} \times 100)$$

$$\text{Heat} = (CVO_2 \times VO_2 + CVCO_2 \times VCO_2)/1000;$$

where $CVO_2 = 3.941$; $CVCO_2 = 1.106$.

Home cage locomotor activity was determined using a multidimensional infrared light beam system.

2.7. Biochemical assays

Blood urea nitrogen (BUN), alanine aminotransferase (ALT), and aspartate aminotransferase (AST) were measured in plasma from mice described in Figures 4–6 and analyzed using the Roche Cobas 8000 clinical chemistry analyzer with a c502 chemistry module. Plasma was collected from trunk blood in the presence of 20 μ L of EDTA (0.5 M, Invitrogen) and insulin was measured using ELISA (Cat. #90080, Crystal Chem, Elk Grove Village, IL). Lipids in plasma and tissue samples from 2 h fasted mice were determined using Infinity™ Triglycerides (Thermo Scientific #TR22421) and Infinity™ Cholesterol (Thermo Scientific #TR13421). Hepatic lipid measurements were conducted following extraction as previously described [38,39].

2.8. Statistics

All data are represented as mean and SEM. Statistical significance was determined using the unpaired Student's *t*-tests or, where appropriate, one-, two-, or three-way ANOVA with multiple comparisons Tukey post-test. ANCOVA was used to evaluate EE changes with respect to lean mass or total body weight. Hill Slope analyses were used to calculate EC50, while Top and Bottom (all % stimulation (cAMP)) refer to the upper and lower plateaus in theses analyses. Significance in all analyses was assigned when $p < 0.05$. Statistical analyses were completed using GraphPad Prism version 9.2 (GraphPad Software, San Diego, CA) or SPSS Statistics (IBM) for Macintosh with the exception of PK.

MOLECULAR METABOLISM

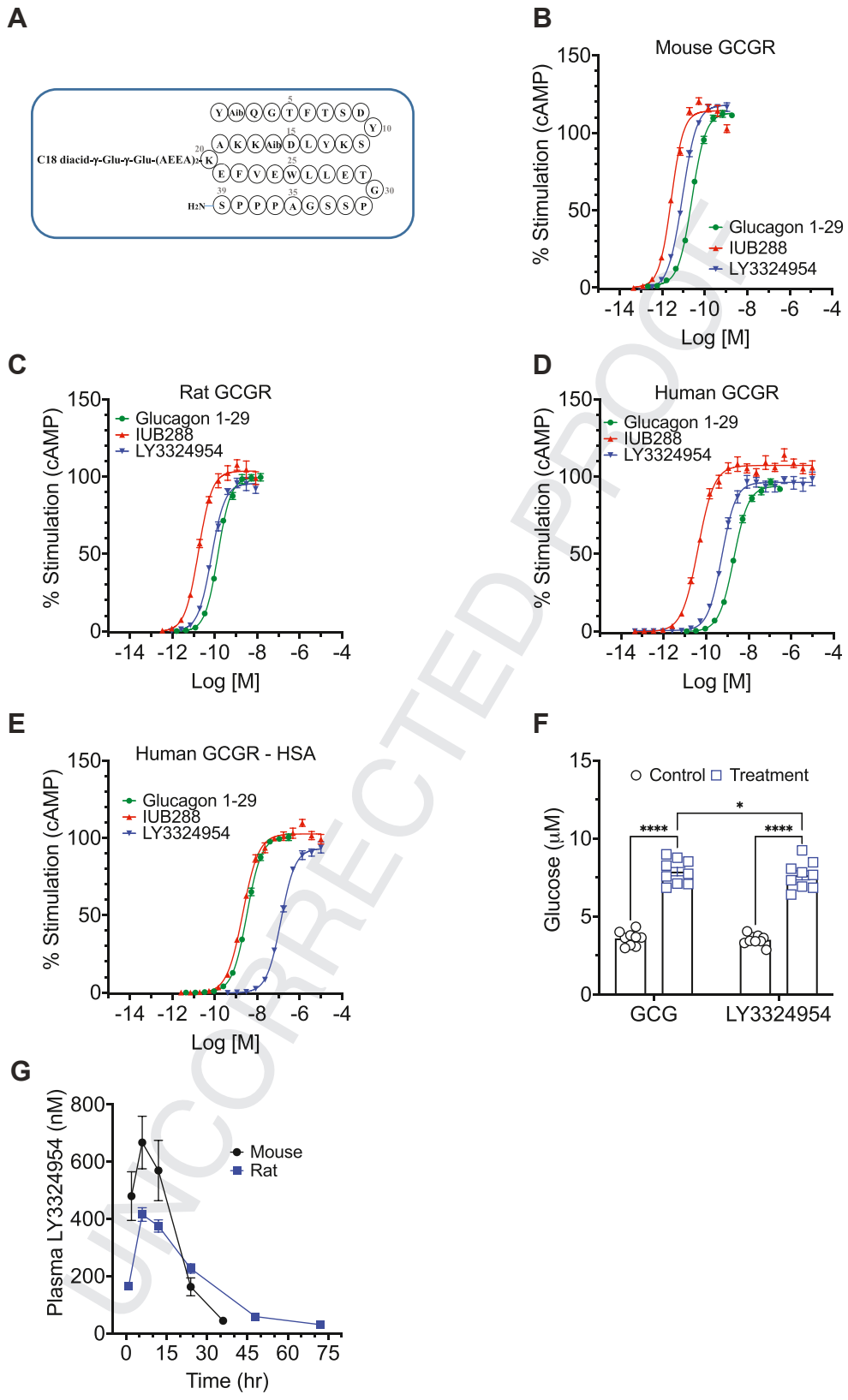

Figure 1: LY3324954 structure and receptor activity. Schematic of LY3324954 primary structure (A). Dose dependent activation (cAMP production) of mouse (B), rat (C), and human (D) GCGR-expressing HEK293 cells when treated with native GCG, IUB288, or LY3324954. Dose dependent activation of human GCGR-expressing HEK293 cells in the presence of medium containing albumin (HSA; E). Glucagon- and LY3324954-stimulated glucose output from human IPSC-derived hepatocytes (F). LY3324954 pharmacodynamics in mouse and rat (G). All data are represented as mean ± SEM. Panels B–F ($n = 8–13$) independent replicates; panel G mice ($n = 4$) and rat ($n = 3$).

Original Article

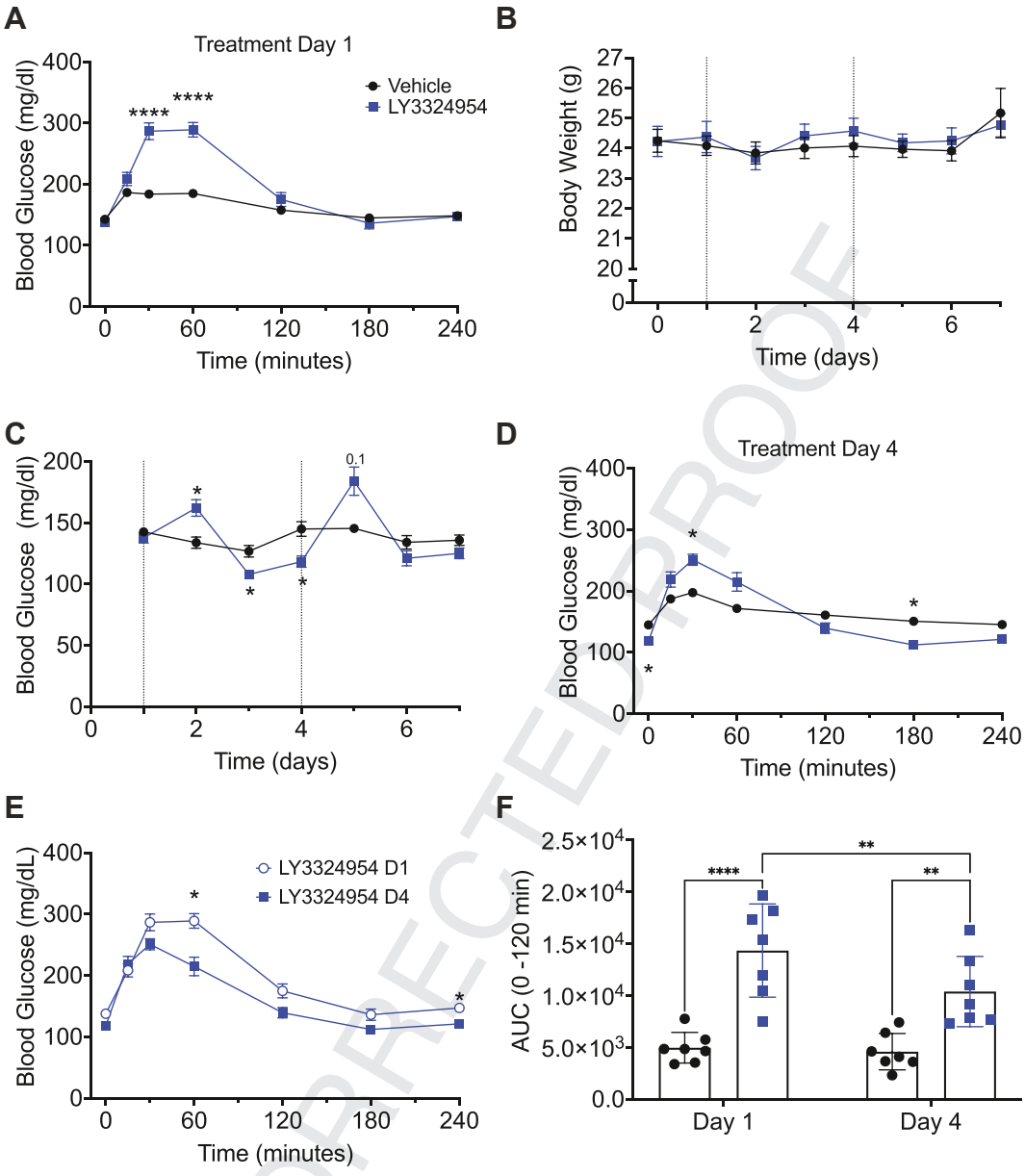

Figure 2: Metabolic response to chronic, long-acting GCGR agonism in lean mice. Blood glucose in response to LY3324954 challenge (day 1, A). Daily body weight (B) and *ad libitum* blood glucose (C) in LY3324954 treated (10 nmol/kg s.c.) mice. Blood glucose in response to second LY3324954 treatment (day 4, D). LY3324954 stimulated glycemic response (E) and area under the curve (AUC) analyses (F) of day 1 or day 4 treatment. Mice treated via sc injection on days 1 and 4 of study. All data are represented as mean ± SEM ($n = 7$) in 10—12-week-old C57Bl/6J mice injected at ZT7 of the light-phase. *$p < 0.05$, **$p < 0.01$, and ****$p < 0.0001$ as analyzed by two-way RM-ANOVA (A—E), or standard two-way ANOVA (F).

Pharmacokinetic parameters were calculated by noncompartmental analysis using Phoenix WinNonlin Version 6.4.

3. RESULTS

3.1. Development of LY3324954 a long-acting and selective GCGR agonist

In an effort to generate a potent, selective, long acting GCGR agonist with enhanced molecule properties, we developed LY3324954. LY3324954 (Figure 1A) is a glucagon analog that contains two non-coded amino acid residues at positions 2, and 16. In addition, the peptide backbone is conjugated to a C18 fatty diacid moiety via a linker/spacer at the position 20 lysine residue, enabling albumin binding as a pharmacokinetic half-life extension strategy while providing desired pharmacological properties.

We validated the activity of LY3324954 at the GCGR via cAMP production in a series of concentration-response studies (Figure 1B—E and Table 1). LY3324954 stimulated cAMP production was assessed from mouse, rat, and human GCGR and was compared to the native glucagon peptide (GCG 1—29) or the known GCGR agonist IUB288 (a C16 fatty monoacid GCGR agonist). All three species of GCGR were more potently activated (i.e., a smaller EC50) by LY3324954 than GCG, but less than IUB288 (Table1). When these studies were repeated in media containing 1% human serum albumin, we

MOLECULAR METABOLISM

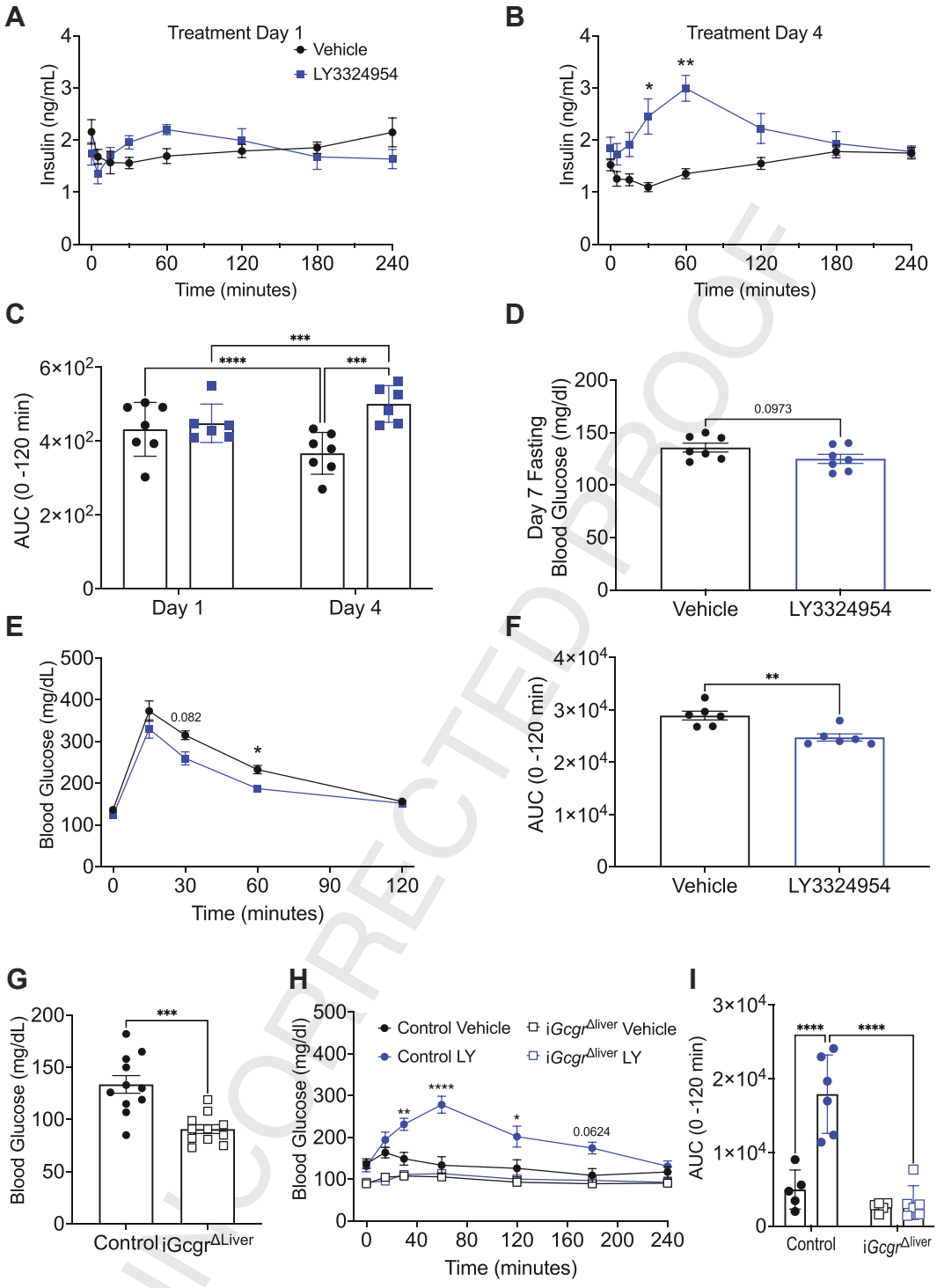

Figure 3: Insulinotropic response to LY3324954 and Glucose Tolerance in lean mice. Plasma insulin excursion in response to day 1 (A) and day 4 (B) of LY3324954 treatments (10 nmol/kg s.c.) and insulin AUC (C). Day 7 fasting blood glucose (D), glucose tolerance test (E, 2 g/kg bw i.p.) and GTT AUC (F). Fasting blood glucose (G, $n = 11$), LY3324954 stimulated glucose excursion (H), and LY3324954 stimulated AUC (I) in control and *iGcgr*$^{\Delta Liver}$ mice. Mice treated via sc injection on days 1 and 4 of study. All data are represented as mean ± SEM. Panels a–f ($n = 6–7$) in 10–12-week-old C57Bl/6J mice from Figure 2 injected at ZT7 of the light-phase. Panels H–I ($n = 5–6$) in 10–12-week-old control and *iGcgr*$^{\Delta Liver}$ mice. *$p < 0.05$, **$p < 0.01$, ***$p < 0.001$, and ****$p < 0.0001$ as analyzed by two-way RM-ANOVA (A,B,E,H), standard two-way ANOVA (C, I), or student's t-test (D,F,G).

Original Article

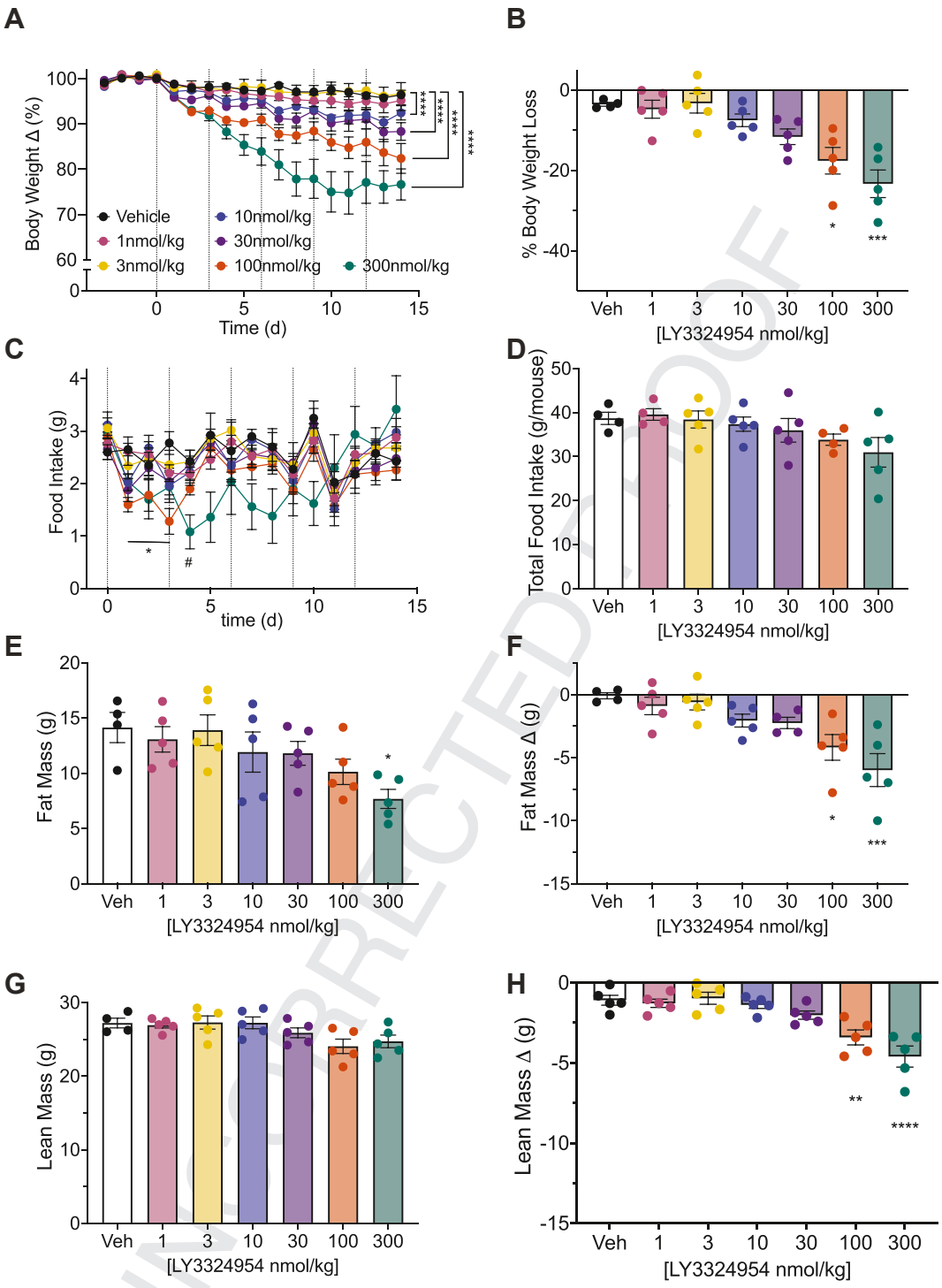

Figure 4: Dose dependent weight loss to LY3324954 treatment in DIO mice. Daily % body weight change (A) and % body weight loss (B) of LY3324954 treated DIO mice. Daily (C) and total (D, 14d) home cage food intake in response to LY3324954 treatment. Day 14 fat mass (E), fat mass change (F, d0-d14), lean mass (G) and lean mass change (H, d0-d14) in LY3324954 treated DIO mice. Dashed vertical lines in panels A and C indicate treatment days. All data are represented as mean ± SEM, ($n = 4$–5) in 22–24-week-old C57Bl/6J mice maintained on HFD for 12 w and injected at ZT11.5 of the light-phase. *$p < 0.05$, **$p < 0.01$, ***$p < 0.001$, and ****$p < 0.0001$ vs vehicle as analyzed by two-way RM-ANOVA (A,B,D) or one-way ANOVA (C,E–H).

observed a right-shift in the concentration-response of LY3324954, and IUB288; consistent with the fatty acid modification and albumin binding of these peptides (Figure 1E). Additional studies in cells specifically expressing the GLP-1R or GIPR demonstrated a high degree of selectivity for the GCGR (Supplemental Figs. 1a–b). Of note, LY3324954 was more selective than IUB288 at the GLP-1R. (~1,700-fold selective vs ~100-fold selective). To assess engagement of the endogenously expressed human GCGR, we modeled glucose output from induced pluripotent stem cell (IPSC)-derived hepatocytes. Incubation with LY3324954 produced similar

MOLECULAR METABOLISM

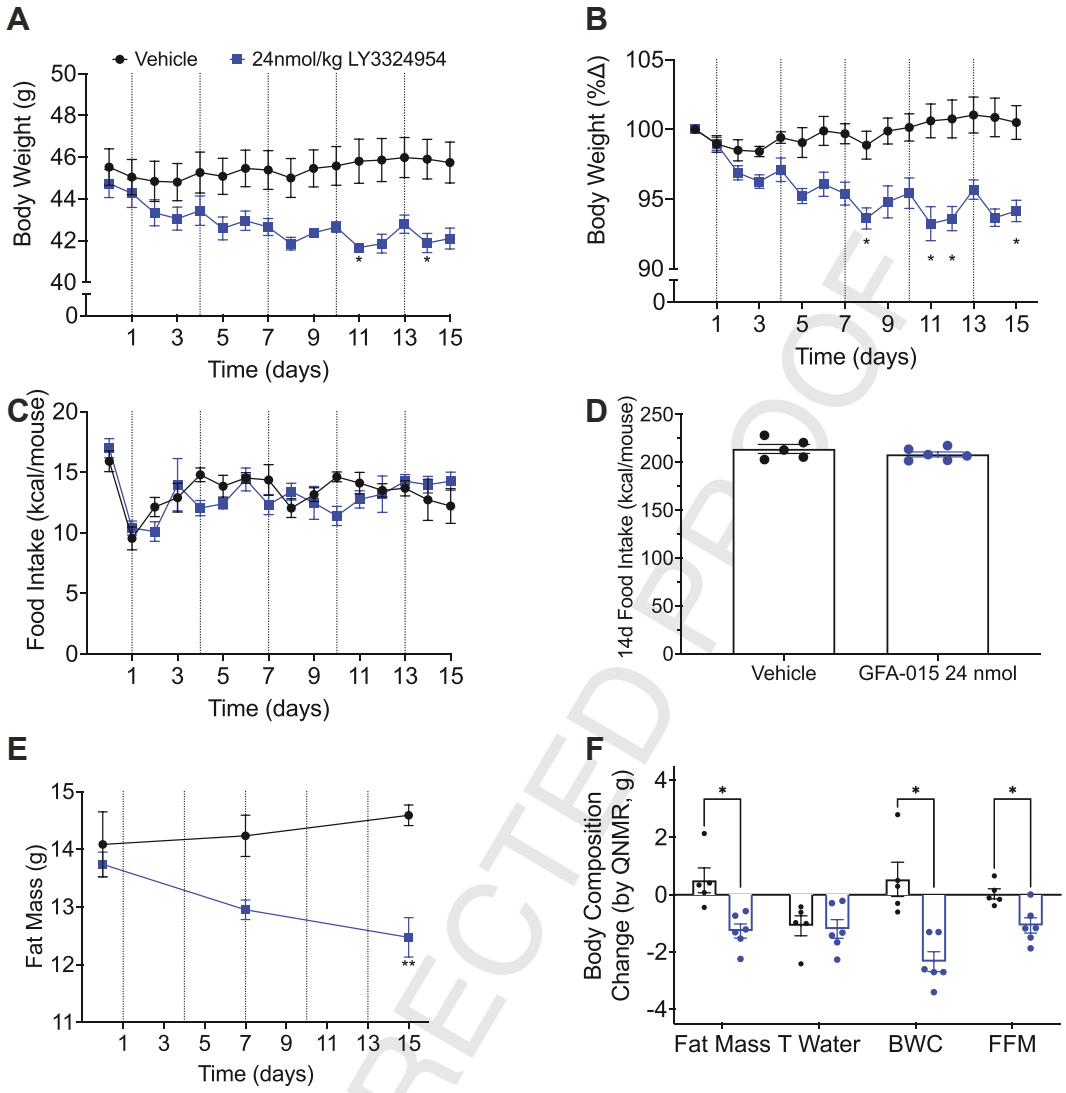

Figure 5: Low dose LY3324954 stimulates weight loss independent of caloric intake in DIO mice. Daily absolute body weight (A) and % body weight change (B) of LY3324954 treated DIO mice (24 nmol/kg sc, every 72 h). Daily food intake (C) and total (15d) food (D) intake measured in TSE calorimeter in response to LY3324954 treatment. Absolute fat mass (E) and body composition change (F) in LY3324954 treated DIO mice. Dashed lines indicate treatment days. All data are represented as mean ± SEM, ($n = 5–6$) in 22–24-week-old C57Bl/6J mice maintained on HFD for 12 w and injected at ZT11.5 of the light-phase. $*p < 0.05$ and $****p < 0.0001$ vs vehicle as analyzed by two-way RM-ANOVA (A–C,E) or student's t-test (D,F).

glucose accumulation in conditioned media as native glucagon (Figure1F).

To determine the PK profile, LY3324954 was assessed in DIO mice, rats, dogs, and monkeys following a single subcutaneous administration. Consistent with the albumin binding effects of acylation, prolonged PK profile of this peptide was observed. Half-life was calculated between 6.5 and 49 h depending upon species (Figure 1G, Table 2). Of note, LY3324954 half-life in rats was 13 h, approximately 2-times longer than that of IUB288 as previously measured in the same species [37]. Together these data demonstrate considerable time extension engineering compared with the approximate 3–6-minute half-life of native glucagon in humans.

3.2. Glycemic response to LY3324954 in lean mice

The robust activation of GCGR and stimulation of hepatocyte glucose output led us to assess the glycemic response to LY3324954 in naïve, chow-fed, lean C57Bl/6J mice over 7d. Subcutaneous injection (10 nmol/kg) of LY3324954 increased blood glucose 30 and 60 min after injection as compared to vehicle treated mice (Figure 2A). This glucose excursion was cleared by 120min and similar glycemia was observed over the next 2 h. Based on the protracted PK of LY3324954 (Figure 1G and Table 2), we administered a second s.c. injection 72 h later (i.e., day 4, depicted as dashed lines in Figure 2B–C) measuring body weight and glycemia every 24 h throughout the study. As expected from our prior studies evaluating chronic GCGR agonism in chow-fed mice [37], LY3324954-treatment did not alter body weight (Figure 2B). LY3324954 administration increased day 2 *ad libitum* glycemia as compared to vehicle-treated controls with a similar trend observed on day 5 ($p = 0.100$, Figure 2C). Interestingly, elevated glycemia on day 2 was followed by 2 days of reduced blood glucose (Figure 2C). Glycemic response to the second injection peaked at 30 min but was followed by a period of reduced glycemia at 180min as

Original Article

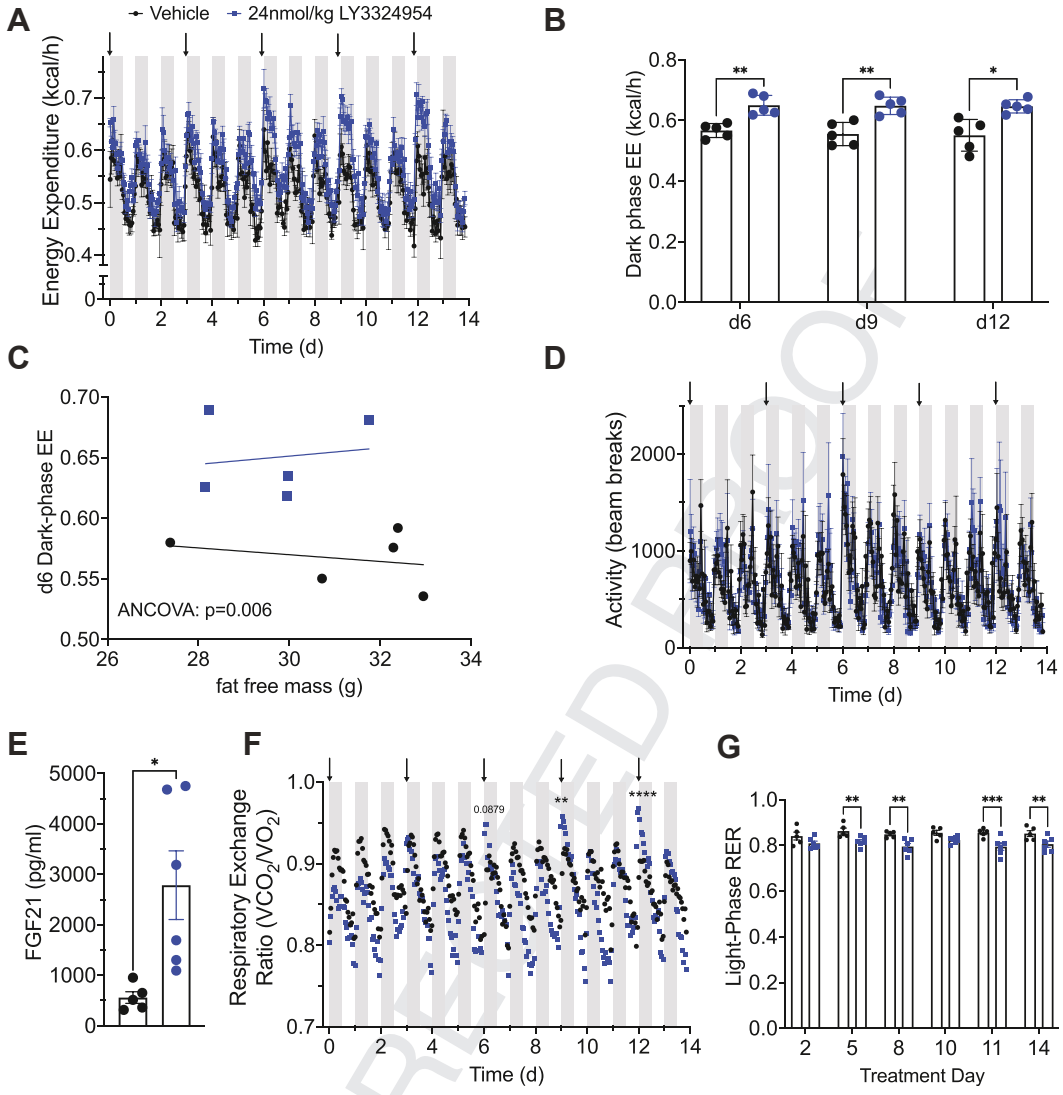

Figure 6: Indirect calorimetry during LY3324954 treatment in DIO mice. Energy expenditure (A—C) and locomotor activity (D) during 14d LY3324954 treatment (24 nmol/kg sc, every 72 h) of mice from Figure 5. Dark phase energy expenditure on days 6, 9, and 12 (B, treatment days) and day 6 expenditure correlated to fat free mass (C). Circulating FGF21 on day 15 of treatment (E). Respiratory exchange ratio (RER) during 14d LY3324954 treatment (F) and light phase RER on days 2, 5, 8, 10, 11, and 14 (G). Data in panels A—B and D—G are represented as mean ± SEM, ($n = 5$) in 22—24 week-old C57Bl/6J mice maintained on HFD for 12 w and injected at ZT11.5 of the light-phase. $^{*}p < 0.05$, $^{**}p < 0.01$, $^{***}p < 0.001$, and $^{****}p < 0.0001$ as analyzed by two-way RM-ANOVA (A, D, F), student's t-test (B, E, G), or ANCOVA (C).

compared to vehicle control mice (Figure 2D). Moreover, as compared to the excursion observed on day 1, the LY3324954 induced glucose excursion was reduced on day 4, as was the area under the curve (Figure 2E—F). Together these data support the chronic *in vivo* regulation of glucose homeostasis following LY3324954 activation of the GCGR.

3.3. LY3324954 stimulated insulin secretion in lean mice

Glucagon and GCGR-agonists are known stimulators of insulin secretion [29,34,35]. Of note, GCGR signaling stimulates hepatic glucose production [1] and β-cell GCGR-signaling enhances glucose-stimulated insulin secretion [29,34,35]. Consistent with these reports, we expected that LY3324954 would stimulate insulin secretion. As anticipated, LY3324954 treatment stimulated a subtle increase in insulin excursion ($p = 0.0019$, interaction of time by treatment) following the initial treatment in lean mice (Figure 3A,C). However, when circulating insulin was assessed in response to the second treatment (day 4), we observed a robust increase as compared to both d4 vehicle-treated or d1 LY3324954 treated mice (Figure 3B—C). This elevated level of circulating insulin likely contributed to the reduced glycemic excursion in response to the second LY3324954 treatment. To assess the effect of chronic GCGR-agonism on glucose homeostasis, we conducted an i.p. glucose tolerance test (ipGTT; 2 g/kg bw). This ipGTT was administered on day 7 in the place of the next LY3324954 treatment. We chose this strategy as it would allow us to separate the chronic effects of GCGR agonism from the increase in circulating insulin we observed following each LY3324954 treatment. We observed a trend for reduced fasting (5 h) glycemia between LY3324954 and vehicle-treated mice ($p = 0.0973$, Figure 3D). Consistent with this trend, we uncovered enhanced glucose tolerance in LY3324954-treated mice as compared to vehicle-controls (Figure 3E—F).

MOLECULAR METABOLISM

Table 1 — Agonist-specific glucagon receptor activation by species.

	Glucagon 1-29	IUB288	LY3324954
Mouse GCGR			
Bottom	1.231	0.1452	−1.327
Top	113.0	114.2	118.0
Log EC50	−10.60	−11.57	−11.05
HillSlope	1.347	1.504	1.283
EC50	2.504e-011	2.687e-012	8.941e-012
Rat GCGR			
Bottom	−0.2761	−0.2635	0.01722
Top	99.55	103.6	95.61
Log EC50	−9.855	−10.77	−10.16
HillSlope	1.430	1.351	1.365
EC50	1.396e-010	1.701e-011	6.858e-011
Human GCGR			
Bottom	−0.1430	−0.3287	0.4969
Top	93.91	107.2	96.27
Log EC50	−8.698	−10.38	−9.262
HillSlope	1.251	1.140	1.317
EC50	2.003e-009	4.168e-011	5.472e-010
Human GCGR in presence of 1% albumin			
Bottom	−0.07247	−0.5594	−0.2627
Top	101.0	102.6	93.22
Log EC50	−8.490	−8.685	−6.888
HillSlope	1.256	1.156	1.289
EC50	3.235e-009	2.064e-009	1.295e-007

Table 2 — Mean pharmacokinetic parameters of LY3324954 following a single subcutaneous dose.

Species	Dose	Tmax	Cmax	$AUC_{0\text{-inf}}$	$T_{1/2}$	CL/F
	nmol/kg	(hour)	(nmol/L)	(hr*nmol/L)	(hour)	(mL/hr/kg)
DIO mouse ($n = 4$)	300	6	668	11899	6.5	25
Rat ($n = 3$)	100	8	425	11692	13	8.8
Dog ($n = 3$)	39	14	303	28077	49	1.4
Monkey ($n = 2$)	50	9	425	31821	44	1.6

Abbreviations: Tmax = time to maximum concentration, Cmax = maximum plasma concentration, AUC0-inf = area under the curve from 0 h to infinity, T1/2 = elimination half-life, CL/F = clearance/bioavailability.

3.4. LY3324954 acts via hepatic GCGR to regulate glucose metabolism in mice

We have previously used hepatic *Gcgr* deficiency ($Gcgr^{\Delta Liver}$) to show that the glucagon analog, IUB288, regulates glucose homeostasis via hepatic GCGR [22,29,30,39]. As a final validation, we assessed LY3324954 in $iGcgr^{\Delta Liver}$ mice. To generate $iGcgr^{\Delta Liver}$ mice we induced AAV-Cre ($Cre^{Thryoxine\text{-}binding\ globulin}$;VB1743; Vector BioLabs) in $Gcgr^{flox/flox}$ mice and treatment was started 7d after induction. Littermate $Gcgr^{flox/flox}$ mice induced with AAV-eGFP were used as controls. Consistent with conditional hepatic Gcgr knockout [29,36], $iGcgr^{\Delta Liver}$ mice were characterized by suppressed *ad libitum* glycemia as compared to control mice (Figure 3G). Importantly, $iGcgr^{\Delta Liver}$ mice were resistant to LY3324954 mediated elevations in blood glucose following acute LY3324954 administration (10 nmol/kg s.c.; Figure 3H—I). Thus, LY3324954 appears to stimulate acute increases in glycemia via mechanisms requiring the liver GCGR.

3.5. Bi-weekly LY3324954 treatments reduce obesity in diet-induced obese (DIO) mice

We have previously reported the anti-obesity effects of GCGR-agonism [22,37,38]. However, GCGR-agonism in those studies was stimulated via IUB288, requiring daily injection. The extended duration of action of LY3324954 allowed us to explore the anti-obesity effects of GCGR-agonism with reduced disturbance to the mice. We conducted a dose response study searching for doses of LY3324954 that would reduce body weight absent of reduced food intake. Prior to treatment C57Bl/6 mice were maintained on 60% high-fat diet (HFD; D12492) for 16 weeks to induce rapid DIO. Mice were switched to 39.7% HFD (TD95217) for 4-8w prior to treatment to facilitate greater dietary sugar and a physiology more relevant to human obesity [40]. Mice were treated every 3d while body weight and food intake were measured daily. We observed a dose-dependent decrease in body weight at doses greater than 30 nmol/kg (Figure 4A—B and Supplemental Fig. 1c). Trends for reduced food intake at higher doses suggest that reduced food intake was likely contributing to this weight loss (Figure 4C—D). Fat mass, and the change in fat mass from day 0—14, were likewise reduced as the LY3324954 dose was increased (Figure 4E—F). Absolute lean mass was similar to that of vehicle-treated control mice, regardless of LY3324954 dose (Figure 4G), while the change in lean mass in grams (Figure 4H) or % lean mass loss (Supplemental Fig. 1d) from day 0—14 was greater at 100 and 300 nmol/kg doses. Plasma analysis at study termination (d14) showed the expected increase in glycemia at higher doses, as well as robust suppression of ALT, plasma cholesterol, and liver triglycerides (Table 3).

Consistent with other GCGR-agonists, LY3324954 stimulated weight loss at doses ≥10 nmol/kg (Figure 4B; $p < 0.01$, 2-way ANOVA). However, unlike the weight loss associated with daily-dosed GCGR-agonists (e.g., IUB288, Supplemental Fig. 3a), food intake was not suppressed until LY3324954 was administered at 100 nmol/kg or more (Figure 4C—D), suggesting the changes in body weight observed at lower doses are due to increased energy expenditure. Thus, indirect calorimetry was conducted in DIO C57Bl/6 mice following 7d of acclimation. Mice were treated with LY3324954 (24 nmol/kg bw) or vehicle every 3d (dashed vertical lines Figure 5A—C) for the duration of a 15d study. This dose was chosen to maximize the energy expenditure effect of GCGR-agonism, while treating below the threshold for

Table 3 — Effects of LY3324954 dose response on biochemical indices in DIO mice.

	Vehicle	1 nmol/kg	3 nmol/kg	10 nmol/kg	30 nmol/kg	100 nmol/kg	300 nmol/kg
Blood glucose (mg/dL)	156.4 ± 9.05	152.9 ± 2.92	152.1 ± 3.63	171.7 ± 9.15	**243.1 ± 13.63****	**258.4 ± 33.15*****	173.4 ± 15.86
BUN (mg/dL)	18.98 ± 0.72	20.32 ± 0.40	21.36 ± 0.84	18.78 ± 2.20	18.08 ± 1.32	18.54 ± 1.65	15.32 ± 2.40
Creatinine (mg/dL)	0.116 ± 0.007	0.118 ± 0.009	0.102 ± 0.006	0.094 ± 0.005	**0.084 ± 0.004***	0.098 ± 0.004	0.09 ± 0.008
ALT (IU/L)	145.8 ± 37.20	**70.6 ± 18.06***	**60.2 ± 9.04***	**68.75 ± 18.03***	**45.4 ± 5.84****	**42.4 ± 3.64****	**52.2 ± 12.21****
AST (IU/L)	163.8 ± 23.88	119 ± 12.48	119 ± 10.01	169.8 ± 24.37	144.0 ± 5.82	107.4 ± 11.63*	169.8 ± 41.02
Chol (mg/dL)	206 ± 15.18	208.8 ± 13.69	196.2 ± 9.28	158.4 ± 21.06	**130.8 ± 8.51****	**102.8 ± 8.33*****	**63.2 ± 4.57*****
Trig (mg/dL)	53.96 ± 8.93	62.48 ± 8.66	66.94 ± 13.13	62.38 ± 9.65	84.88 ± 19.33	61.32 ± 13.16	96.14 ± 21.66
Liver trig (mg/g)	157 ± 50.08	143.5 ± 35.26	110.7 ± 27.17	**37.43 ± 13.38***	**14.22 ± 3.94****	**6.49 ± 0.90****	**7.52 ± 0.60****

Samples collected approximately 24 h after the last LY3324954 injection, at the end of the light cycle, and under *ad libitum* conditions in $n = 5$ mice/group.

its hypophagic action. LY3324954 stimulated weight loss was independent of changes in food intake (Figure 5A–D), yet reduced fat mass and fat-free mass from day 0 to day 15 (Figure 5E–F).

Consistent with isocaloric weight loss, we observed increased energy expenditure in LY3324954-treated DIO mice (Figure 6A–C). Specifically, LY3324954 treatment increased energy expenditure across the 14d treatment period ($p = 0.0003$, time by treatment interaction). Moreover, there was a robust response to treatments on days 6, 9, and 12, suggesting a progressive accumulation of the molecular processes that drive this expenditure (Figure 6A–C). Energy expenditure was not correlated with either lean mass (Figure 6C) or body weight (Supplemental Fig. 2) suggesting these co-variates were insufficient to explain the increased expenditure. As in our prior studies with IUB288 [22], energy expenditure did not increase immediately after the first LY3324954 injection but appears to build over the first week of treatment (Figure 6A). Whether this is due to the biology of GCGR signaling, or the pharmacodynamics of these long acting GCGR-agonists is unknown. Home-cage activity was not altered by treatment (Figure 6D); however, we did observe a robust increase in circulating FGF21 (Figure 6E), which likely contributed to the increased energy expenditure [22,37,38]. Together these data support that low doses of LY3324954 reduce body weight and adiposity via increased energy expenditure in DIO mice.

Respiratory exchange ratio (RER; VCO_2/VO_2) was also measured during this 14d treatment. Like energy expenditure, LY3324954 treatment elevated RER in the hours immediately after treatment (Figure 6F). Intriguingly, we observed reduced light-phase RER on 6 of the 14 days measured (Figure 6G). This suggests that GCGR-agonism enhances carbohydrate oxidation in the periods immediately following treatment, but also enhances lipid oxidation during the animal's resting period, where food intake is naturally lower.

Upon study termination we assessed circulating factors contributing to glucose and lipid homeostasis. As expected, we observed elevated blood glucose in LY3324954-treated mice (Table 4). Plasma triglycerides were likewise elevated, but liver triglycerides were considerably reduced (Table 4). Plasma cholesterol levels were also reduced suggesting that lipid homeostasis is benefited by chronic GCGR agonism in this DIO model (Table 4). Consistent with improved liver function, circulating ALT was reduced and AST was unchanged by LY3324954 treatment (Table 4). LY3324954 treatment also reduced BUN and creatinine levels in these mice (Table 4).

In a subsequent cohort of DIO mice, we evaluated the anti-obesity effects of LY3324954 (10 nmol/kg; bi-weekly) as compared to IUB288 (10 nmol/kg; daily). Consistent with Figure 4, this LY3324954 dose had no effect on food intake, but stimulated weight loss in DIO mice (Supplemental Figs. 3a–g). Weight loss in IUB288-treated mice was similar over the first 10d of the study (Supplemental Fig. 3c). The two treatments separated in the final days (d11-16) as IUB288 reduced food intake (Supplemental Figs. 3a–g). Both treatments induced a subtle decrease in lean mass; however, this effect was only significant with IUB288 treatment (Supplemental Fig. 3h).

Similar to effects in lean mice (Figure 2), subcutaneous injection (10 nmol/kg) of LY3324954 increased blood glucose 30 and 60 min after a single injection (Day 1; Supplemental Fig. 3i). This excursion was similar that observed in the IUB288-treated mice. Similar effects were also observed on Day 4 (Supplemental Fig. 3k). Plasma insulin from study termination (day 16) uncovered reduced circulating insulin in both LY3324954- and IUB288-treated mice as compared to vehicle controls. Together these data support a role for enhanced insulin action and confirm our earlier reports on chronic GCGR-agonism.

Table 4 — Effects of 24 nmol/kg LY3324954 on biochemical indices in DIO mice.

	Vehicle	24 nmol/kg
Blood glucose (mg/dL)	161.2 ± 13.17	**217.8 ± 13.57***
BUN (mg/dL)	22.90 ± 2.28	**18.30 ± 1.40***
Creatinine (mg/dL)	0.122 ± 0.005	**0.100 ± 0.003***
ALT (IU/L)	130.5 ± 14.08	**69.00 ± 14.12***
AST (IU/L)	127.7 ± 5.67	124.0 ± 21.00
Chol (mg/dL)	218.0 ± 5.07	**144.0 ± 8.16****
Trig (mg/dL)	33.03 ± 4.82	**54.18 ± 4.18****
Liver trig (mg/g)	264.5 ± 11.22	**50.87 ± 8.09****

Samples collected approximately 24 h after the last LY3324954 injection, at the end of the light cycle, and under *ad libitum* conditions in $n = 6$ mice/group.

4. DISCUSSION

Results presented here characterize LY3324954, a novel GCGR-agonist, in lean and diet-induced obese mice. These data add to the accumulating reports of GCGR-agonists and their metabolic effects. GCGR activity was previously assumed to oppose insulin actions, resulting in many attempts to antagonize this receptor [41]. However, emerging observations suggest that GCGR stimulation may integrate with insulin [29,32]. Intriguingly, GLP1/GCGR and GLP1/GIP/GCG multi-agonists display the lipolytic and thermogenic properties of GCGR agonism [23,24,27,42]. However, the incretin actions of GIPR and GLP-1R agonism in these peptides control the hyperglycemic effect of glucagon [23,24,27,42]. Importantly, these peptides also have longer half-lives than native glucagon. The temporal regulation of GCGR activation may influence this crosstalk, thus optimized tools to probe GCGR action will be of great value. Our findings here support that GCGR-agonists with extended duration of action, administered on a biweekly basis, retain the metabolic benefits observed in shorter-acting peptides.

This study utilized multiple rodent and humanized cell models to expand our understanding of extended GCGR signaling on energy balance and glucose homeostasis. We and others have previously reported the effects of GCGR agonism to enhance insulin secretion [29,43]. Glucagon is known to enhance glucose-stimulated insulin secretion (GSIS) via direct agonism of both β-cell GCGR and β-cell GLP-1R (reviewed in [43]). While both receptors are sufficient for this incretin-like response, GLP-1R activation appears to be the dominate pathway for glucagon's insulinotropic actions [43]. In the current report we show that the GCGR agonist LY3324954 stimulated transient glucose excursions in lean and DIO mice. These excursions were were dependent on hepatic GCGR signaling and accompanied by increased circulating insulin in lean mice. This is of interest as prior reports suggest that kidney gluconeogenesis is sufficient to compensate for complete ablation of hepatic glucose production (via hepatic deletion of the glucose-6-phosphatase gene) [44]. Future tracer-based studies are needed to elucidate the contribution of kidney gluconeogensis in LY3324954-mediated glucose homeostasis.

Intriguingly, LY3324954-stimulated glucose excursions appear to diminish with subsequent dosing. Conversely, LY3324954-associated insulin excursions in lean mice increased with additional exposures. Importantly, this treatment did not induce steady-state hyperglycemia, but rather mice displayed trends for reduced fasting glycemia and enhanced glucose tolerance on study-day 7. Thus, we interpret these findings to suggest that GCGR-agonism enhances insulin secretion and improves glucose homeostasis, even with longer-acting GCG peptides.

MOLECULAR METABOLISM

The anti-obesity effects of GCGR agonism are gaining considerable appreciation [45]. Consistent with these effects, LY3324954 reduced body weight and fat mass in a dose-dependent manner. It is of great interest whether the well-established catabolic effects of GCGR agonism on amino acids [46] will translate to reduced skeletal muscle mass and function. We did not observe profound changes in absolute lean mass in our studies, even at the highest doses. It should be noted that changes day 0 to day 14 lean mass (Δg) were detected at doses of 100 and 300 nmol/kg. Conversely, the considerable effects of GCGR-agonism to reduce fat mass suggest that an effective dose that targets fat mass loss and preserves lean mass can be expected. This hypothesis is supported by the observation of LY3324954 stimulated energy expenditure and subsequent weight loss in the absence of reduced food intake. This observation is of interest as increased expenditure is usually accompanied by increased caloric intake. Our data support that the benefits of GCGR-stimulated energy expenditure are absent of changes to food intake, at lower doses, and may be enhanced when some degree of hypophagia is concurrently induced. Increased energy expenditure following GCGR-agonist, IUB288, is dependent on hepatic GCGR expression [22]. This regulation involves direct effects of the liver via Farnesoid X Receptor (FXR) as well as liver-brain signaling transmitted via FGF21 signaling at its receptor, β-Klotho, in neurons of the brain [22,38]. Whether IUB288 or any other peripherally delivered GCGR-agonist stimulates direct signaling via neuronal GCGR or the roles of other potential thermogenic signals (e.g., epinephrine, T3, T4) have yet to be elucidated. We expect that LY3324954 stimulates similar hepatic and extrahepatic signaling, and together these findings suggest a mechanistic benefit of glucagon receptor agonism in the context of multi-agonist that reduce food intake [24,27].

Beyond energy expenditure and reduction of fat mass our study confirmed a profound lipid-lowering effect in LY3324954 treated DIO mice. DIO mice exhibit increased liver triglycerides, dyslipemia (including increased circulating cholesterol), and insulin resistance; all components of Metabolic dysfunction-associated steatotic liver disease (MASLD). LY3324954-induced reductions in circulating cholesterol and liver tiglycerides were coupled to considerable reduction in the liver transaminase ALT. Together this cluster of markers support a reversal of MASLD in the DIO mouse.

Gcgr is expressed in kidney nephrons with the greatest levels of expression and activity localized to the thick ascending limbs where they may act to regulate renal urea, electrolyte, potassium and glucose homeostasis [47]. BUN and Creatinine levels are elevated in obesity [48,49] yet were suppressed by LY3324954 treatment; suggesting that the benefits of chronic GCGR-agonism may extend to kidney function as has been recently implicated [50]. While reduced creatinine may suggest kidney dysfunction BUN was also reduced and thus, the BUN/Cr ratio in LY-treated mice was similar to that of controls ($p = 0.14$). We interpreted these data to support a normal physiologic adaptation to increased GCGR-signaling.

This study also used a known, long-acting GCGR-agonist, IUB288. Although less potent at the GCGR, LY3324954 has a longer half-life and better selectivity than IUB288. Regardless of these pharmacological differences, both GCGR-agonists exhibited similar stimulation of acute glucose excursion and profound anti-obesity effects in DIO mice. Intriguingly, the weight loss in LY3324954 at this dose was independent of changes in food intake. This subtle difference may be associated with the reduced activity of this peptide at the GLP-1R or with the protracted activation of the GCGR.

These current findings add to the reagents targeting GCGR activity. These peptides allow for nuanced interrogation of GCGR-dependent physiology. Consistent with this benefit, our studies bolster the emerging appreciation of GCGR in the regulation of energy balance, lipid, and glucose metabolism. Collectively these studies provide deeper mechanistic understanding to the benefits observed in GCGR-based coagonists [23–25,27,42]. Our studies also provide additonal insight for the application of bihormonal (GCG and insulin), bionic pancreas devices [51]. In sum, these data suggest that extended GCGR agonism (e.g., LY3324954) retains the metabolic benefits of short-acting peptides and is useful for interrogation of mechanisms underlying long-acting glucagon-based therapies.

CRediT AUTHORSHIP CONTRIBUTION STATEMENT

William Roell: Writing — review & editing, Writing — original draft, Methodology, Investigation, Conceptualization. **Tamer Coskun:** Writing — review & editing, Writing — original draft, Project administration, Methodology, Investigation, Formal analysis, Data curation, Conceptualization. **Teayoun Kim:** Methodology, Investigation, Formal analysis, Data curation. **Libbey O'Farrell:** Methodology, Investigation. **Jennifer A. Martin:** Methodology, Investigation. **Shelly Nason:** Methodology, Investigation. **Jasmin Hernandez-Alamillo:** Methodology, Investigation. **Saidharshana Dhantu:** Methodology, Investigation. **Daniel J. Drucker:** Writing — review & editing, Resources. **Kyle W. Sloop:** Writing — review & editing, Resources, Methodology, Investigation, Conceptualization. **James P. Steele:** Methodology, Investigation. **Jorge Alsina-Fernandez:** Writing — review & editing, Writing — original draft, Resources, Methodology, Investigation, Conceptualization. **Kirk M. Habegger:** Writing — review & editing, Writing — original draft, Visualization, Resources, Project administration, Methodology, Investigation, Funding acquisition, Formal analysis, Data curation, Conceptualization.

ACKNOWLEDGEMENTS

The project described was supported by the NIH grants 1R01DK112934 (KMH), 1R01DK137506 (KMH), and P30DK079626, and by the Lilly Research Award Program (WR and KMH). DJD is supported by a Banting and Best Diabetes Centre Novo Nordisk Chair in Incretin biology and a Sinai Health Novo Nordisk Foundation Fund in regulatory peptides.

WR,TC, JH-A, and KMH were responsible for study conception and design, data analyses and interpretation, and drafting the article; TK, LO'F, JM, JH-A, DD, KS, JS, SN, and JA-F generated experimental data; DJD, KS, and JS advised study concept and critical revision of the article. KMH is the guarantor of this work and, as such, had full access to all the data in the study and takes responsibility for the integrity of the data and the accuracy of the data analysis.

DECLARATION OF COMPETING INTEREST

The authors declare the following financial interests/personal relationships which may be considered as potential competing interests: Kirk Habegger reports financial support and equipment, drugs, or supplies were provided by Eli Lilly and Company. Kirk Habegger reports a relationship with Eli Lilly and Company that includes: funding grants. If there are other authors, they declare that they have no known competing financial interests or personal relationships that could have appeared to influence the work reported in this paper.

Original Article

APPENDIX A. SUPPLEMENTARY DATA

Supplementary data to this article can be found online at https://doi.org/10.1016/j.molmet.2024.102073.

DATA AVAILABILITY

Data will be made available on request.

REFERENCES

[1] Habegger KM, Heppner KM, Geary N, Bartness TJ, DiMarchi R, et al. The metabolic actions of glucagon revisited. Nat Rev Endocrinol 2010;6(12):689—97.

[2] Muller TD, Finan B, Clemmensen C, DiMarchi RD, Tschop MH. The new biology and pharmacology of glucagon. Physiol Rev 2017;97(2):721—66.

[3] Eaton RP. Hypolipemic action of glucagon in experimental endogenous lipemia in the rat. J Lipid Res 1973;14(3):312—8.

[4] Hagen JH. Effect of glucagon on the metabolism of adipose tissue. J Biol Chem 1961;236:1023—7.

[5] Lefebvre P. Glucagon and adipose tissue. Biochem Pharmacol 1975;24(13—14):1261—6.

[6] Richter WO, Robl H, Schwandt P. Human glucagon and vasoactive intestinal polypeptide (VIP) stimulate free fatty acid release from human adipose tissue *in vitro*. Peptides 1989;10(2):333—5.

[7] Vaughan M. Effect of hormones on glucose metabolism in adipose tissue. J Biol Chem 1961;236:2196—9.

[8] Vaughan M, Steinberg D. Effect of hormones on lipolysis and esterification of free fatty acids during incubation of adipose tissue in vitro. J Lipid Res 1963;4:193—9.

[9] Gerich JE, Lorenzi M, Bier DM, Schneider V, Tsalikian E, et al. Prevention of human diabetic ketoacidosis by somatostatin. Evidence for an essential role of glucagon. N Engl J Med 1975;292(19):985—9.

[10] Prip-Buus C, Pegorier JP, Duee PH, Kohl C, Girard J. Evidence that the sensitivity of carnitine palmitoyltransferase I to inhibition by malonyl-CoA is an important site of regulation of hepatic fatty acid oxidation in the fetal and newborn rabbit. Perinatal development and effects of pancreatic hormones in cultured rabbit hepatocytes. Biochem J 1990;269(2):409—15.

[11] Pegorier JP, Garcia-Garcia MV, Prip-Buus C, Duee PH, Kohl C, et al. Induction of ketogenesis and fatty acid oxidation by glucagon and cyclic AMP in cultured hepatocytes from rabbit fetuses. Evidence for a decreased sensitivity of carnitine palmitoyltransferase I to malonyl-CoA inhibition after glucagon or cyclic AMP treatment. Biochem J 1989;264(1):93—100.

[12] Weick BG, Ritter S. Dose-related suppression of feeding by intraportal glucagon infusion in the rat. Am J Physiol 1986;250(4 Pt 2):R676—81.

[13] Salter JM. Metabolic effects of glucagon in the Wistar rat. Am J Clin Nutr 1960;8:535—9.

[14] Holloway SA, Stevenson JA. Effect of glucagon on food intake and weight gain in the young rat. Can J Physiol Pharmacol 1964;42:867—9.

[15] Martin JR, Novin D. Decreased feeding in rats following hepatic-portal infusion of glucagon. Physiol Behav 1977;19(4):461—6.

[16] Le Sauter J, Geary N. Hepatic portal glucagon infusion decreases spontaneous meal size in rats. Am J Physiol 1991;261(1 Pt 2):R154—61.

[17] Joel CD. Stimulation of metabolism of rat brown adipose tissue by addition of lipolytic hormones *in vitro*. J Biol Chem 1966;241(4):814—21.

[18] Kuroshima A, Yahata T. Thermogenic responses of brown adipocytes to noradrenaline and glucagon in heat-acclimated and cold-acclimated rats. Jpn J Physiol 1979;29(6):683—90.

[19] Davidson IW, Salter JM, Best CH. The effect of glucagon on the metabolic rate of rats. Am J Clin Nutr 1960;8:540—6.

[20] Davidson IW, Salter JM, Best CH. Calorigenic action of glucagon. Nature 1957;180(4595):1124.

[21] Song KH, Chiang JY. Glucagon and cAMP inhibit cholesterol 7alpha-hydroxylase (CYP7A1) gene expression in human hepatocytes: discordant regulation of bile acid synthesis and gluconeogenesis. Hepatology 2006;43(1):117—25.

[22] Kim T, Nason S, Holleman C, Pepin M, Wilson L, et al. Glucagon receptor signaling regulates energy metabolism via hepatic farnesoid X receptor and fibroblast growth factor 21. Diabetes 2018;67(9):1773—82.

[23] Day JW, Ottaway N, Patterson JT, Gelfanov V, Smiley D, et al. A new glucagon and GLP-1 co-agonist eliminates obesity in rodents. Nat Chem Biol 2009;5(10):749—57.

[24] Finan B, Yang B, Ottaway N, Smiley DL, Ma T, et al. A rationally designed monomeric peptide triagonist corrects obesity and diabetes in rodents. Nat Med 2015;21(1):27—36.

[25] Jastreboff AM, Kaplan LM, Frias JP, Wu Q, Du Y, et al. Triple-hormone-receptor agonist retatrutide for obesity - a phase 2 trial. N Engl J Med 2023.

[26] Rosenstock J, Frias J, Jastreboff AM, Du Y, Lou J, et al. Retatrutide, a GIP, GLP-1 and glucagon receptor agonist, for people with type 2 diabetes: a randomised, double-blind, placebo and active-controlled, parallel-group, phase 2 trial conducted in the USA. Lancet 2023;402(10401):529—44.

[27] Coskun T, Urva S, Roell WC, Qu H, Loghin C, et al. LY3437943, a novel triple glucagon, GIP, and GLP-1 receptor agonist for glycemic control and weight loss: from discovery to clinical proof of concept. Cell Metabol 2022;34(9):1234—1247 e9.

[28] Unger RH, Madison LL, Muller WA. Abnormal alpha cell function in diabetics response to insulin. Diabetes 1972;21(5):301—7.

[29] Kim T, Holleman CL, Nason S, Arble DM, Ottaway N, et al. Hepatic glucagon receptor signaling enhances insulin-stimulated glucose disposal in rodents. Diabetes 2018;67(11):2157—66.

[30] Kim T, Nason S, Antipenko J, Finan B, Shalev A, et al. Hepatic mTORC2 signaling facilitates acute glucagon receptor enhancement of insulin-stimulated glucose homeostasis in mice. Diabetes 2022;71(10):2123—35.

[31] Gray SM, Goonatilleke E, Emrick MA, Becker JO, Hoofnagle AN, et al. High doses of exogenous glucagon stimulate insulin secretion and reduce insulin clearance in healthy humans. Diabetes 2024;73(3):412—25.

[32] Besse-Patin A, Jeromson S, Levesque-Damphousse P, Secco B, Laplante M, et al. PGC1A regulates the IRS1:IRS2 ratio during fasting to influence hepatic metabolism downstream of insulin. Proc Natl Acad Sci U S A 2019;116(10):4285—90.

[33] Perry RJ, Zhang D, Guerra MT, Brill AL, Goedeke L, et al. Glucagon stimulates gluconeogenesis by INSP3R1-mediated hepatic lipolysis. Nature 2020;579(7798):279—83.

[34] Svendsen B, Larsen O, Gabe MBN, Christiansen CB, Rosenkilde MM, et al. Insulin secretion depends on intra-islet glucagon signaling. Cell Rep 2018;25(5):1127—1134 e2.

[35] Capozzi ME,WJ, Koech J, Gordon AN, Coch RW, Svendsen B, Finan B, et al. Glucagon lowers glycemia when β-cells are active. JCI Insight 2019;5(16):e129954.

[36] Longuet C, Robledo AM, Dean ED, Dai C, Ali S, et al. Liver-specific disruption of the murine glucagon receptor produces alpha-cell hyperplasia: evidence for a circulating alpha-cell growth factor. Diabetes 2013;62(4):1196—205.

[37] Habegger KM, Stemmer K, Cheng C, Muller TD, Heppner KM, et al. Fibroblast growth factor 21 mediates specific glucagon actions. Diabetes 2013;62(5):1453—63.

[38] Nason SR, Antipenko J, Presedo N, Cunningham SE, Pierre TH, et al. Glucagon receptor signaling regulates weight loss via central KLB receptor complexes. JCI Insight 2021;6(4).

[39] Nason SR, Kim T, Antipenko JP, Finan B, DiMarchi R, et al. Glucagon-receptor signaling reverses hepatic steatosis independent of leptin receptor expression. Endocrinology 2020;161(1).

MOLECULAR METABOLISM

[40] Speakman JR. Use of high-fat diets to study rodent obesity as a model of human obesity. Int J Obes 2019;43(8):1491–2.
[41] Scheen AJ, Paquot N, Lefebvre PJ. Investigational glucagon receptor antagonists in Phase I and II clinical trials for diabetes. Expet Opin Invest Drugs 2017;26(12):1373–89.
[42] Nahra R, Wang T, Gadde KM, Oscarsson J, Stumvoll M, et al. Effects of cotadutide on metabolic and hepatic parameters in adults with overweight or obesity and type 2 diabetes: a 54-week randomized phase 2b study. Diabetes Care 2021;44(6):1433–42.
[43] El K, Capozzi ME, Campbell JE. Repositioning the alpha cell in postprandial metabolism. Endocrinology 2020;161(11).
[44] Mutel E, Gautier-Stein A, Abdul-Wahed A, Amigo-Correig M, Zitoun C, et al. Control of blood glucose in the absence of hepatic glucose production during prolonged fasting in mice: induction of renal and intestinal gluconeogenesis by glucagon. Diabetes 2011;60(12):3121–31.
[45] Zeigerer A, Sekar R, Kleinert M, Nason S, Habegger KM, et al. Glucagon's metabolic action in Health and disease. Compr Physiol 2021;11(2):1759–83.
[46] Winther-Sorensen M, Galsgaard KD, Santos A, Trammell SAJ, Sulek K, et al. Glucagon acutely regulates hepatic amino acid catabolism and the effect may be disturbed by steatosis. Mol Metabol 2020;42:101080.
[47] Bankir L, Bouby N, Blondeau B, Crambert G. Glucagon actions on the kidney revisited: possible role in potassium homeostasis. Am J Physiol Ren Physiol 2016;311(2):F469–86.
[48] Chang AR, Zafar W, Grams ME. Kidney function in obesity-challenges in indexing and estimation. Adv Chron Kidney Dis 2018;25(1):31–40.
[49] Kjaergaard AD, Teumer A, Witte DR, Stanzick KJ, Winkler TW, et al. Obesity and kidney function: a two-sample mendelian randomization study. Clin Chem 2022;68(3):461–72.
[50] Wang MY, Zhang Z, Zhao S, Onodera T, Sun XN, et al. Downregulation of the kidney glucagon receptor, essential for renal function and systemic homeostasis, contributes to chronic kidney disease. Cell Metabol 2024;36(3):575–597 e7.
[51] Russell SJ, El-Khatib FH, Sinha M, Magyar KL, McKeon K, et al. Outpatient glycemic control with a bionic pancreas in type 1 diabetes. N Engl J Med 2014;371(4):313–25.

